

Nickel-based phosphide superconductor with infinite-layer structure, BaNi₂P₂

Takashi Mine ¹, Hiroshi Yanagi ¹, Toshio Kamiya ^{1,2}, Yoichi Kamihara ², Masahiro Hirano ^{2,3}, and Hideo Hosono ^{1,2,3,*}

¹ *Materials and Structures Laboratory, Tokyo Institute of Technology, 4259 Nagatsuta, Midori-ku, Yokohama 226-8503, Japan*

² *ERATO-SORST, JST, in Frontier Research Center, Tokyo Institute of Technology, 4259 Nagatsuta, Midori-ku, Yokohama 226-8503, Japan*

³ *Frontier Research Center, Tokyo Institute of Technology, 4259 Nagatsuta, Midori-ku, Yokohama 226-8503, Japan*

Abstract

Analogous to cuprate high- T_c superconductors, a NiP-based compound system has several crystals in which the Ni-P layers have different stacking structures. Herein, the properties of BaNi₂P₂ are reported. BaNi₂P₂ has an infinite-layer structure, and shows a superconducting transition at ~3 K. Moreover, it exhibits metallic conduction and Pauli paramagnetism in the temperature range of 4 – 300 K. Below 3 K, the resistivity sharply drops to zero, and the magnetic susceptibility becomes negative, while the volume fraction of the superconducting phase estimated from the diamagnetic susceptibility reaches ~100 vol.% at 1.9 K. These observations substantiate that BaNi₂P₂ is a bulk superconductor.

Keywords: A. Superconductor; D. Electronic transport

PACS: 74.25.Fy, 74.25.Ha, 74.70.Dd

Footnotes:

(*) Tel: +81-45-924-5359
FAX: +81-45-924-5339
E-mail: hosono@msl.titech.ac.jp

1. Introduction

Cu- and other transition metal-based compounds are attractive for exploring high-transition-temperature (high- T_c) superconductors because it is considered that the high transition temperatures benefit from the strong electron correlation between 3d electrons in the transition metal atoms. Many cuprate high- T_c superconductors have been discovered, including one reported in 1993, which has T_c of 133 K [1]. On the other hand, typical T_c 's of other transition metal based compounds (including oxides and pnictides) are lower than those of cuprate high- T_c superconductors. However, the discovery of new classes of superconductors, such as Sr_2RuO_4 [2], $\text{Na}_x\text{CoO}_2 \cdot y\text{H}_2\text{O}$ [3], electron-doped HfNCl [4], Li_xNbO_2 [5], has provided complementary insight to better understand the mechanism of superconductivity as well as clues for exploring higher- T_c materials.

Recently, we have studied a series of quaternary compounds, which contain transition metal ions, $\text{La}T_M\text{OP}_n$ (T_M = transition-metal cations such as Mn, Fe, Ni, and Co; Pn = P and As), with the expectation that this series will be a new correlated electron system. In our studies, we have found new superconductors, LaFeOP_n [6, 7] and LaNiOP_n [8, 9], and an itinerant ferromagnet, LaCoOP_n [10]. As shown in Fig. 1(a), $\text{La}T_M\text{OP}_n$ has a layered crystal structure where the positively charged La-O layers and negatively charged $T_M\text{-P}_n$ layers, which are composed of an edge-sharing network of $T_M\text{P}_n$ tetrahedra, are alternately stacked along the c axis. It is thought that the $T_M\text{-P}_n$ layers sandwiched between the wider-gap La-O layers form magnetic and carrier conduction layers.

Ternary compounds containing transition metal ions, $AT_{M2}\text{P}_2$ (A = Ca, Sr, Ba, and lanthanide cations), have the ThCr_2Si_2 structure and belong to the $I4/nmm$ space group. In addition, these ternary compounds show unusual physical properties such as intermediate valence states (EuNi_2P_2 [11]) and various magnetic properties, ranging from Pauli paramagnetism (CaNi_2P_2 [12]) to ferromagnetism (LaCo_2P_2 [11]), and to antiferromagnetism (CaCo_2P_2 [13]). Figure 1 (b) shows the crystal structure of $AT_{M2}\text{P}_2$, which has a layered structure similar to $\text{La}T_M\text{OP}$. The structure of the $T_M\text{-P}$ layer is essentially the same as that in $\text{La}T_M\text{OP}$ where the $T_M\text{-P}$ layers are composed of an edge-sharing network of $T_M\text{P}_4$ tetrahedra. However, the wider-gap La-O layers in $\text{La}T_M\text{OP}$ are replaced with the A cation layers in $AT_{M2}\text{P}_2$. Thus, this crystal structure lacks a wider-gap insulating layer. Therefore, this structure may be regarded as an infinite-layer structure, which is analogous to cuprate high- T_c superconductors. Because an infinite-layer cuprate, $(\text{Sr}_{1-x}\text{Ca}_x)_{1-y}\text{CuO}_2$, exhibits a high- T_c of 110 K [14], we speculate that superconducting transitions are present in infinite-layer compounds composed of other transition metal cations, $ANi_2\text{P}_2$ and $AFe_2\text{P}_2$. Although to date, $AFe_2\text{P}_2$ (A = Ca, Sr, Ba, La) and $ANi_2\text{P}_2$ (A = Ca, La) have been examined, a superconducting transition has not been observed down to 1.8 K [12, 15]. Only LaRu_2P_2 with the ThCr_2P_2 -type structure shows a superconducting transition at 4.1 K [15].

Here we report that a ThCr_2Si_2 -type phosphide, BaNi_2P_2 , exhibits a superconducting

transition at \sim 3 K. Although Keimes et al. [16] have previously synthesized BaNi_2P_2 and reported its crystal structure, they did not report its electrical and magnetic properties. We synthesized \sim 90% pure BaNi_2P_2 samples, and measured their electrical and magnetic properties down to 1.9 K.

2. Experimental

Samples were prepared by a solid-state reaction of the starting materials, Ba (Johnson Matthey Company, 99.9%), P (Rare Metallic, 99.9999%), and Ni (Nilaco Corporation, 99.9%). A stoichiometric mixture of the Ba, P, and Ni powders was pressed into a pellet, and heated in an evacuated silica tube initially at 400 °C for 12 h and then at 1000 °C for 12 h. The sintered pellet was reground and subsequently pressed into a pellet, which was sintered at 1000 °C for 12 h. The resulting samples were characterized by high-power X-ray diffraction (XRD, D8 ADVANCE-TXS, Bruker AXS) with Cu K α radiation, which detected trace amounts of impurity phases, BaNi_9P_5 , $\text{Ba}(\text{PO}_3)_2$, and $\text{BaNi}_2(\text{PO}_4)_2$. Therefore, the crystal structure of BaNi_2P_2 and the compositions of the impurities were refined by the four-phase Rietveld method using the code TOPAS3 [17].

Electrical resistivity of the sintered pellets (apparent densities: \sim 63%) were measured in the temperature range from 1.9 to 300 K by the four-probe technique (using PPMS, Quantum Design). Sputtered Au films were used as ohmic contacts. Magnetic measurements were carried out using a vibrating sample magnetometer (VSM, using PPMS, Quantum Design). Temperature dependence of the magnetization was measured in a magnetic field at 10 Oe after zero-field cooling (ZFC) to the measurement temperatures.

3. Results and discussion

Figure 2 shows the powder XRD pattern of the purest sample obtained to date, which still shows diffraction peaks of BaNi_2P_2 , BaNi_9P_5 , $\text{Ba}(\text{PO}_3)_2$, and $\text{BaNi}_2(\text{PO}_4)_2$. Four-phase Rietveld analyses revealed that the obtained sample was mainly BaNi_2P_2 , but contained \sim 9 vol.% of BaNi_9P_5 , \sim 2 vol.% of $\text{Ba}(\text{PO}_3)_2$, and \sim 1 vol.% of $\text{BaNi}_2(\text{PO}_4)_2$. The obtained samples are dark gray and chemically stable in air.

Figure 3 shows the temperature dependence of the electrical resistivity (ρ) at an external magnetic field (H) of 0 Oe. The resistivity at 300 K was 2.8 m Ω ·cm, and a metallic behavior was observed at temperatures down to \sim 3 K. The inset shows a magnified view in the temperature range of 1.9 – 10 K as a function of H . At $H = 0$ Oe, ρ dropped sharply at \sim 3 K, and the resistivity vanished at 2.7 K, implying a superconducting transition. The onset temperature where ρ begins to drop decreases as H increases, and the drop in ρ vanishes at $H = 1000$ Oe. These results suggest that the observed changes are due to a superconducting transition at \sim 3 K.

Figure 4 shows the temperature dependence of the mass magnetization (M) measured at 10

Oe after the ZFC. M was as small as $\sim 1 \times 10^{-4}$ emu/g, and was nearly independent of temperature at 4 – 300 K, implying Pauli paramagnetism in this temperature range. However, M began to drop, became negative at ~ 3 K, and reached a large negative value of -1.1×10^{-1} emu/g at 1.9 K. These results, together with the zero resistance in Fig. 3, clearly indicate that the obtained sample exhibits superconductivity at temperatures below ~ 3 K. The field dependence of the magnetization (M - H) curve in the inset of Fig. 4 shows that the decrease in the negative magnetization is proportional to H at $H < 150$ Oe, and then increases to zero as H increases up to 550 Oe. This behavior is similar to that observed in type-II superconductors. Furthermore, in this case the lower and upper critical magnetic fields were estimated to be $H_{c1} = \sim 150$ Oe and $H_{c2} = \sim 550$ Oe, respectively. The volume fraction of the superconducting phase estimated from the slope of the M - H curve at $H < 150$ Oe was nearly 100%.

Next, the effects of the impurity phases were assessed. The impurity phase BaNi_9P_5 shows a temperature-independent Pauli paramagnetism [18], whereas $\text{BaNi}_2(\text{PO}_4)_2$ exhibits an antiferromagnetic transition at a Neel temperature of 24 K [19]. Rietveld analyses showed that the volume fractions of the impurity phases [~ 9 vol.% for BaNi_9P_5 , ~ 1 vol.% for $\text{BaNi}_2(\text{PO}_4)_2$, and ~ 2 vol.% for $\text{Ba}(\text{PO}_3)_2$] were negligible compared to that of the superconducting phase. Consequently, we conclude that BaNi_2P_2 is a bulk superconductor below ~ 3 K. Although other Ni-based superconductors, $Ln\text{Ni}_2\text{B}_2\text{C}$ ($Ln = \text{Y}, \text{Tm}, \text{Er}, \text{Ho}, \text{and Lu}$) and $\text{La}_3\text{Ni}_2\text{B}_2\text{N}$, which are composed of tetrahedral Ni layers similar to LaNiOP_n and BaNi_2P_2 , have been reported, each Ni ion is coordinated not by P_n , but by B ions [20, 21]. It is known in crystal chemistry and complex chemistry that Cu^{2+} ions tend to take planar four coordinate structures, while Ni and Fe ions prefer to take tetrahedral structures, suggesting that a planar Cu^{2+} structure is not a requisite for superconductivity, and such a transition metal-based tetrahedral layer is key to discovering new superconductors.

4. Summary

BaNi_2P_2 , which belongs to the $AT_{M2}\text{P}_2$ system with the ThCr_2Si_2 structure, is regarded as an infinite-layer structure. BaNi_2P_2 shows a superconducting transition at ~ 3 K. Thus, BaNi_2P_2 is tentatively assigned as a type-II superconductor with a lower critical magnetic field of ~ 150 Oe and an upper field of ~ 550 Oe at 1.9 K. In the $AT_{M2}\text{P}_2$ system, the transition metal T_M can be replaced with other transition metal ions, and the lattice parameters can also be controlled by replacing the A cation. These features provide a new platform to systematically survey the relationship among superconducting transitions, d electron configurations, and crystal structures. Hence, the discovery of higher- T_c superconductors is anticipated in this and related material systems.

References

- [1] A. Schilling, M. Cantoni, J. D. Guo, H. R. Ott, *Nature* 363 (1993) 56.
- [2] Y. Maeno, H. Hashimoto, K. Yoshida, S. Nishizaki, T. Fujita, J. G. Bednorz, F. Lichtenberg, *Nature* 372 (1994) 532.
- [3] K. Takada, H. Sakurai, E. Takayama-Muromachi, F. Izumi, R. A. Dilanian, T. Sasaki, *Nature* 422 (2003) 53.
- [4] S. Yamanaka, K. Hotohama, H. Kawaji, *Nature* 392 (1998) 580.
- [5] M. J. Geselbracht, T. J. Richardson, A. M. Stacy, *Nature* 345 (1990) 324.
- [6] Y. Kamihara, H. Hiramatsu, M. Hirano, R. Kawamura, H. Yanagi, T. Kamiya, H. Hosono, *J. Am. Chem. Soc.* 128 (2006) 10012.
- [7] Y. Kamihara, T. Watanabe, M. Hirano, H. Hosono, *J. Am. Chem. Soc.* 130 (2008) 3296.
- [8] T. Watanabe, H. Yanagi, T. Kamiya, Y. Kamihara, H. Hiramatsu, M. Hirano, H. Hosono, *Inorg. Chem.* 46 (2007) 7719.
- [9] T. Watanabe, H. Yanagi, Y. Kamihara, T. Kamiya, M. Hirano, H. Hosono, *J. Solids State Chem.* (2008), doi:10.1016/j.jssc.2008.04.033.
- [10] H. Yanagi, R. Kawamura, T. Kamiya, Y. Kamihara, M. Hirano, T. Nakamura, H. Osawa, H. Hosono, (submitted).
- [11] E. Mörsen, B. D. Mosel, W. Müller-Warmuth, M. Reehuis, W. Jeitschko, *J. Phys. Chem. Solids* 49 (1988) 785.
- [12] W. Jeitschko, M. Reehuis, *J. Phys. Chem. Solids* 48 (1987) 667.
- [13] M. Reehuis, W. Jeitschko, G. Kotzyba, B. Zimmer, X. Hu, *J. Alloys Compd.* 266 (1998) 54.
- [14] M. Azuma, Z. Hiroi, M. Takano, Y. Bando, Y. Takeda, *Nature* 356 (1992) 775.
- [15] W. Jeitschko, R. Glaum, L. Boonk, *J. Solid State Chem.* 69 (1987) 93.
- [16] V. Keimes, D. Johrendt, A. Mewis, C. Huhnt, W. Schlabitz, *Anorg. Allg. Chem.* 623 (1997) 1699.
- [17] Bruker AXS. TOPAS, version 3, Bruker AXS, Karlsruhe, Germany, 2005.
- [18] J. V. Badding, A. M. Stacy, *J. Solid State Chem.* 87 (1990) 10.
- [19] L. P. Regnault, J. Y. Henry, J. Rossat-Mignod, A. De Combarieu, *J. Magn. Magn. Mat.* 15-18 (1980) 1021.
- [20] R. J. Cava, H. Takagi, H. W. Zandbergen, J. J. Krajewski, W. F. Peck Jr, T. Siegrist, B. Batlogg, R. B. Van Dover, R. J. Felder, K. Mizuhashi, J. O. Lee, H. Eisaki, S. Uchida, *Nature* 367 (1994) 252.
- [21] R. J. Cava, H. W. Zandbergen, B. Batlogg, H. Eisaki, H. Takagi, J. J. Krajewski, W. F. Peck Jr, E. M. Gyorgy, S. Uchida, *Nature* 372 (1994) 245.

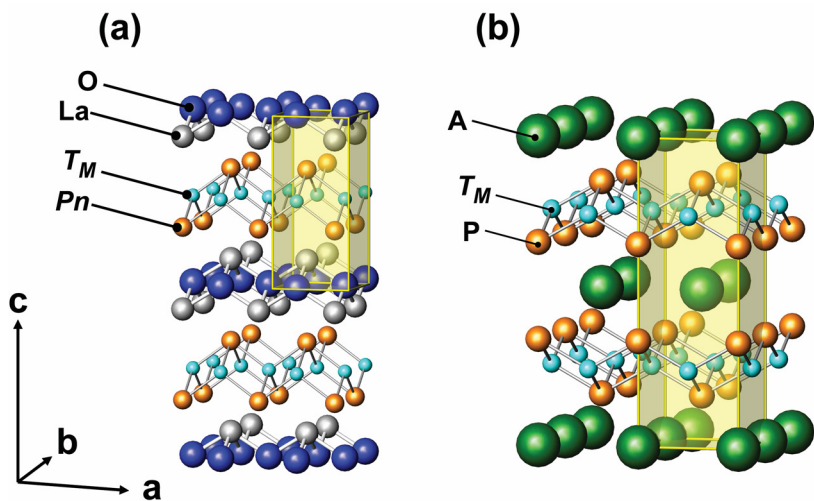


Fig. 1. (a) Crystal structure of LaT_MOPn . La-O layers and $T_M\text{-P}n$ layers are stacked along the c axis. (b) Crystal structure of $AT_{M2}\text{P}_2$. Structure of the $T_M\text{-P}$ layer is similar to that in LaT_MOP .

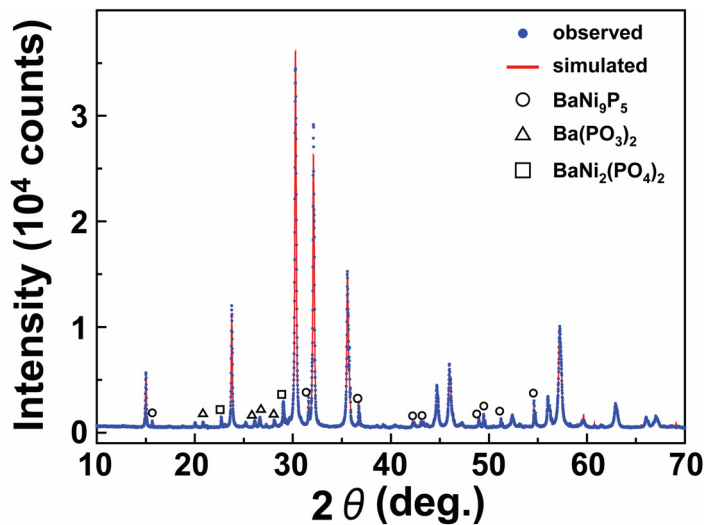


Fig. 2. XRD pattern of BaNi_2P_2 sample measured (blue circles) and simulated by the Rietveld method using the refined result (red line). Trace amounts of impurities, BaNi_9P_5 , $\text{Ba}(\text{PO}_3)_2$, and $\text{BaNi}_2(\text{PO}_4)_2$, are detected, and their diffraction peaks are indicated by open circles, triangles, and squares, respectively.

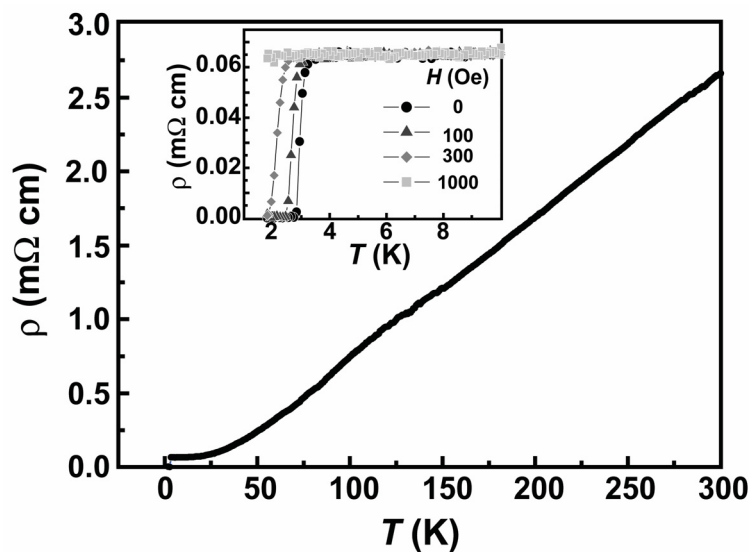


Fig. 3. Temperature (T) dependence of the electrical resistivity (ρ) at $H = 0$ Oe. Inset shows the ρ - T curves as a function of H magnified in the temperature range of 1.9–10 K.

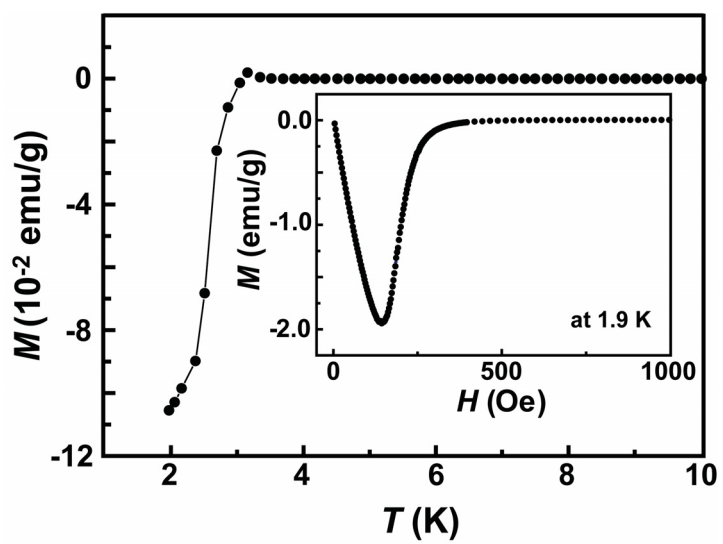


Fig. 4. Temperature (T) dependence of the mass magnetization (M) measured at 10 Oe after cooling to 1.9 K under a zero magnetic field. Inset shows the field (H) dependence of M at 1.9 K.